Highly conductive Sb-doped layers in strained Si

N. S. Bennett,[a] N. E. B. Cowern, A. J. Smith, R. M. Gwilliam, and B. J. Sealy
Advanced Technology Institute, University of Surrey, Guildford GU2 7XH, United Kingdom

L. O'Reilly and P. J. McNally
Nanomaterials Processing Laboratory, RINCE, School of Electronic Engineering, Dublin City University, Dublin 9, Ireland

G. Cooke and H. Kheyrandish
CSMA-MATS, Queens Road, Stoke on Trent, Stafford shire ST4 7LQ, United Kingdom

(Received 1 September 2006; accepted 23 September 2006; published online 3 November 2006)

The ability to create stable, highly conductive ultrashallow doped regions is a key requirement for future silicon-based devices. It is shown that biaxial tensile strain reduces the sheet resistance of highly doped *n*-type layers created by Sb or As implantation. The improvement is stronger with Sb, leading to a reversal in the relative doping efficiency of these *n*-type impurities. For Sb, the primary effect is a strong enhancement of activation as a function of tensile strain. At low processing temperatures, 0.7% strain more than doubles Sb activation, while enabling the formation of stable, ~10-nm-deep junctions. This makes Sb an interesting alternative to As for ultrashallow junctions in strain-engineered complementary metal-oxide-semiconductor devices. © *2006 American Institute of Physics*. [DOI: 10.1063/1.2382741]

Strain engineering has become an essential approach to meet performance requirements of metal-oxide-semiconductor devices on Si.[1] While the role of strain in channel mobility enhancement is well recognized,[2] little is known about its effects on the behavior of dopant atoms, such as those in ultrashallow source/drain extensions. Scaling requirements for ultrashallow junctions include reducing junction depth and increasing junction steepness, while keeping sheet resistance—inversely related to carrier mobility, activation, and junction depth—low despite the narrower current path allowed by the scaled junction.[1]

Arsenic is the favored *n*-type dopant species for *n*-channel source/drain doping in conventional Si. Experimental literature discussing As implants in bulk and strained Si layers has shown sheet resistance to be reduced under tensile strain. This was reported to be a result of mobility enhancement, with *no* evidence to date for any improvement in activation.[3,4] On the other hand, theoretical calculations by Sadigh *et al.* have suggested that biaxial tensile strain should have large effects on the solubility of dopant atoms, and that solid solubility limits can be increased by several orders of magnitude for large *n*-type species implanted into tensile strained silicon, a combined result of dopant size mismatch and strain effects on the Fermi level.[5] Although there have been a number of experimental attempts to test this prediction in recent years, none has so far shown a significant positive result.

Due to its greater nuclear stopping power and lower range straggle, Sb is favorable compared to As with respect to its as-implanted "metallurgical" junction depth and junction abruptness. Previously we have shown that implanted Sb can be highly activated in conventional unstrained Si following low-temperature thermal processing, with very little out diffusion for temperatures $<800\ ^\circ\mathrm{C}$.[6,7] If strain does indeed improve Sb solid solubility,[5] it is in strain-engineered devices that Sb may be best utilized. Coupled with this is the processing benefit that Sb diffusion is retarded in the presence of tensile strain,[8] whereas As diffusion appears to be increased.[9]

In this letter we report on experiments that replicate—in one dimension—the proposed formation of Sb source/drain extension regions in biaxial tensile strained silicon. Our study compared IQE Silicon Compounds wafers with 17.5 nm strained Si layers, grown on $Si_{0.83}Ge_{0.17}$ relaxed buffer layers, with conventional *p*-type Si control wafers. Defect-free growth on relaxed buffer layers with 17% Ge content will create a strain level of 0.7% in the strained Si layer, and micro-Raman spectroscopy measurements confirmed that the layers were indeed strained to this level.

Both the strained and unstrained wafers underwent the same processing sequence, as follows. Each wafer was implanted with low energy (2 keV) Sb or As to a dose of $3.5\times10^{14}\ \mathrm{cm}^{-2}$, creating as-implanted junctions at 12 or 14 nm, respectively, as defined at the $3\times10^{18}\ \mathrm{cm}^{-3}$ level. Implant doses were confirmed by Rutherford backscattering spectroscopy and secondary-ion-mass spectrometry (SIMS), and junction depths were determined by SIMS. The SIMS measurements were performed using a 500 eV Cs^+ analyzing beam, giving a sputter-limited depth resolution of ~2 nm/decade, essential to resolve the details of the ultrashallow Sb profiles generated in this work.

After implantation the wafers were cut into pieces and activated using a 10 s isochronal annealing cycle in the range of 600–800 °C. Subsequently, samples were examined using further high-resolution SIMS and van der Pauw sheet resistance measurements combined with Hall-effect measurements to measure active carrier density and Hall mobility throughout the implanted region.[10]

The measured van der Pauw sheet resistance (R_s) of the *n*-type layers is shown in Fig. 1 as a function of annealing temperature. Sb implants into conventional Si show similar resistance characteristics to those found by Alzanki *et al.*[6] where the lowest R_s is seen for processing at 600 and 700 °C, and R_s increases as the anneal temperature is raised to 800 °C and above. Figure 1(a) illustrates the considerable

[a]Electronic mail: nicholas.bennett@surrey.ac.uk

 © 2006 American Institute of Physics
Downloaded 30 Jan 2008 to 136.206.1.17. Redistribution subject to AIP license or copyright; see http://apl.aip.org/apl/copyright.jsp

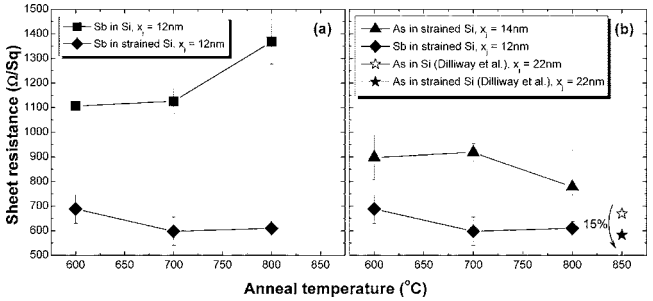

FIG. 1. R_s measurements as a function of annealing temperature (10 s RTA) for 2 keV, 3.5×10^{14} cm^{-2} implants. (a) Sb in Si and strained Si. (b) As and Sb in strained Si. The As results are compared with data from Dilliway *et al.* (Ref. 4), which show a 15% reduction in R_s in the case of 3 keV, 4×10^{14} cm^{-2} As implants in bulk and strained Si.

reduction in R_s (a factor of up to 2.5) for Sb in strained compared to unstrained Si. Just as in conventional Si, the best R_s value is found at low processing temperatures, here, 700 °C. However, in contrast to conventional Si, R_s remains stable as the anneal temperature is raised to 800° C, an important practical advantage for industrial processing.

Figure 1(b) compares results obtained for Sb and As implants under the same processing conditions. The reader can see that for these low anneal temperatures Sb produces more highly conducting layers, even though the Sb junctions are expected to be shallower than the As ones. The shallower junctions for Sb are a result of (a) the shallower Sb-implanted distribution and (b) the absence of transient enhanced diffusion (TED), which is an important feature in the case of As. For processing at 800 °C the R_s for As implants tends to improve towards the Sb case. At this temperature, however, Dilliway *et al.* have shown that As exhibits very significant strain-enhanced TED and other diffusion effects.[4] This led to a junction depth ~80% deeper than that reported for Sb in the present letter. It is also noteworthy that the results in Ref. 4 [presented for comparison in Fig. 1(b)] show only a 15% R_s improvement between the strained and unstrained cases for 3 keV, 4×10^{14} cm^{-2} As implants into strained Si on a $Si_{0.8}Ge_{0.2}$ strain-relaxed buffer.

Figure 2(a) illustrates the areal density (or "dose") of active carriers (N_s) measured by the Hall-effect technique. For Sb implants in bulk Si, the best levels of activation are seen after processing at 600 and 700 °C, in agreement with previous findings.[6,7] Comparing Sb implants in bulk Si with those in the strained case, the figure demonstrates that the strain has more than doubled the amount of electrically active Sb. At 600 and 700 °C, activation is improved from 30% to 60%. Likewise in Fig. 2(b), it can be seen that for identical implants in the strained material, Sb is more highly

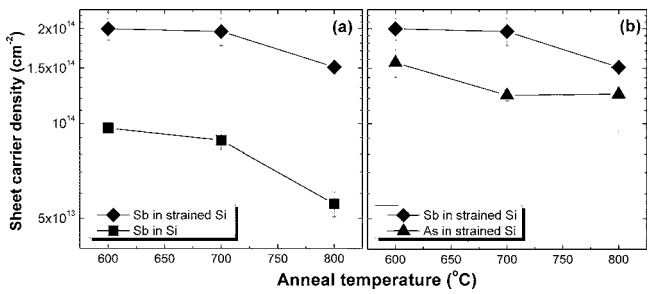

FIG. 2. N_s measurements as a function of annealing temperature (10 s RTA) for the 2 keV, 3.5×10^{14} cm^{-2} Sb and As implants shown in Fig. 1.

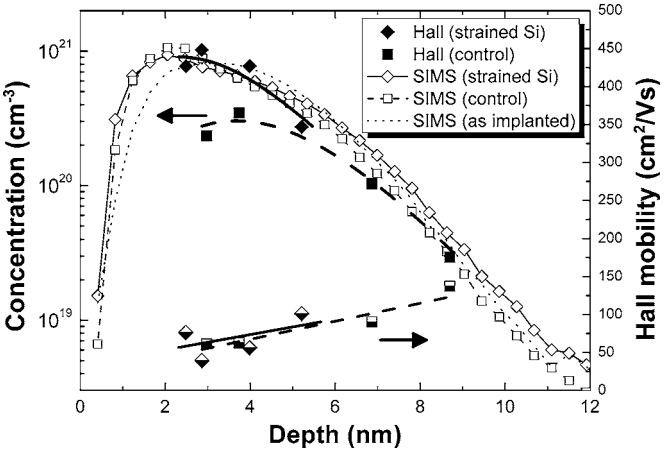

FIG. 3. SIMS and differential Hall profiles for Sb-implanted strained and unstrained silicon (2 keV, 3.5×10^{14} cm^{-2}) followed by RTA (10 s at 700 °C). The thin dotted curve is the as-implanted Sb atomic profile. The thin curves connecting the open symbols are Sb atomic profiles after annealing. The filled symbols are electrically active Sb concentrations after annealing, and the partly filled symbols are the corresponding mobilities. The thick curves through the electrical data are provided as a guide to the eye. In all cases, continuous curves are results for strained Si and the dashed curves are for unstrained Si.

activated than As for low-temperature processing.

This is the first time that a reduction in R_s in tensile strained Si has been shown to be a result of an enhancement in electrical activation. Previous work on As has suggested that activation is unchanged.[3,4] Modest reductions in R_s were reported, but the available data indicated that these were only a result of increased mobility.[3,4] Although the carrier density is subject to a currently unknown correction factor due to scattering mechanisms inherent in the Hall-effect measurement,[11] it seems unlikely that this will discount the activation effect. Evaluating the literature, the reduction in R_s which we have demonstrated seems much too large to be a result of mobility enhancement.[12]

Having shown the benefits of Sb in terms of overall electrical activation, we now turn to a comparison of the chemical and electrical *profiles* of Sb in both strained and unstrained Si. In Fig. 3, the dotted curve and the curves with open symbols show SIMS profiles of Sb after implantation, and after annealing for 10 s at 700 °C—the condition which gave the best value of R_s. The data show that the junction depth of 12 nm is not significantly increased by this anneal. This is consistent with previous observations of the annealing of implanted Sb in unstrained Si, where no movement was found in the tail of the Sb profile.[7] In the peak region of the Sb profile, some movement does occur, consistent with redistribution of Sb towards the surface and a modest degree of pileup at or near the Si/SiO_2 interface (located at ~2 nm nominal depth in Fig. 3). This behavior is apparent in both the strained and unstrained Si, although the pileup is marginally reduced in the strained case. A similar redistribution behavior, in unstrained Si, has been observed by Sealy *et al.* using medium-energy ion scattering measurements.[13]

Figure 3 also shows the corresponding electrical profiles in strained and unstrained Si after annealing. Active carrier concentration (filled symbols) and mobility (half-filled symbols) were both measured by the differential Hall technique.[10] Results shown are corrected for surface depletion,[14] enabling the Sb electrical and atomic profiles to be properly matched with respect to depth. Carrier concen-

Downloaded 30 Jan 2008 to 136.206.1.17. Redistribution subject to AIP license or copyright; see http://apl.aip.org/apl/copyright.jsp

tration and mobility values are left as measured, and would thus be subject to correction if the Hall scattering factor were not equal to 1. The electrically active profile of Sb in strained Si reaches a peak level of $\sim 10^{21}$ cm^{-3}, comparable to the peak atomic concentration measured by SIMS. On the other hand, the electrical profile for Sb in unstrained Si reaches a much lower peak level of $\sim 3 \times 10^{20}$ cm^{-3}, implying that a substantial proportion of the Sb in the peak region is electrically inactive—presumably in the form of clusters or precipitates.

Currently little work has been done on the Hall scattering correction factor for electrons in strained material; however, literature on holes suggests that a value of ~ 0.5 is not unreasonable.[15] Correcting in such a way would have the effect of reducing the Sb carrier concentration peak while increasing Hall mobility. However, it would not be easy to justify theoretically such a large increase in mobility with strain, when the concentration of charged scattering centers in the strained material is at least 5×10^{20} cm^{-3}, thus presumably damping out the contribution of band gap changes to mobility. According to this argument a scattering factor close to unity, as we have used in Fig. 3, would appear more plausible. It is also worth noting that even with a correction factor of 0.5, we would still have a nearly 70% increase in peak Sb activation combined with a mobility doubling as a result of strain.

Currently full reasoning for our activation effect is not offered, but we may consider two possible explanations. The first is a donor ionization effect whereby more Sb is ionized in the strained substrate as a result of strain-induced conduction-band lowering. Temperature-dependent Hall and van der Pauw measurements were carried out to search for such an effect, but the results suggest that Sb, already a very shallow donor in silicon, is not affected by strain in this way. We believe that the most likely explanation is an increased level of Sb solubility in the strained silicon. This interpretation is supported, although somewhat indirectly, by reports of enhanced activation of B in Si driven by *compressive* strain.[16,17] In this case, where the lattice strain field is compressive and the local strain field around the relatively small substitutional B atom is tensile, B activation is seen to be increased. This increase is attributed to a compensation effect between the two strain fields, favoring substitutional incorporation of B. In our experiments substitutional Sb, being a larger atom than Si, would similarly relieve the tensile lattice strain field in our experiment. This, together with band gap effects,[5] could account for the increased activation of Sb seen in the present study. Why such an effect has not previously been seen for As is not clear, but several suggestions are possible.

(1) The As concentrations used were well above the threshold for As cluster formation, but below the solid solubility with respect to second-phase formation (precipitation).
(2) The layers used, being thicker than the Matthews-Blakeslee critical thickness,[18] might have caused unforeseen effects arising from higher defect densities.
(3) Following the strain compensation argument, the lattice mismatch between As and Si is too small to cause a significant change in solubility.

In summary, large sheet resistance improvements for Sb-doped layers produced in strained silicon have been presented. Doping with Sb is seen to produce more highly conductive layers than with As, as a consequence of combined improvements in mobility and dopant activation between the strained and unstrained case. For low-temperature processing, strain is shown to significantly improve the activation of Sb atoms while creating stable ultrashallow junctions to a depth of ~ 10 nm. The results suggest that Sb might be a superior alternative to As for creating ultrashallow junctions in strain-engineered complementary metal-oxide-semiconductor devices.

The authors would like to acknowledge IQE Silicon Compounds Ltd. for providing the strained silicon substrates used in these experiments. Part of this work has been supported by the European Union within the framework of the IST-ATOMICS project.

[1] The International Technology Roadmap for Semiconductors 2005.
[2] F. Schaffler, Semicond. Sci. Technol. **12**, 1515 (1997).
[3] N. Sugii, S. Irieda, J. Morioka, and T. Inada, J. Appl. Phys. **96**, 261 (2004).
[4] G. D. M. Dilliway, A. J. Smith, J. J. Hamilton, J. Benson, L. Xu, P. J. McNally, G. Cooke, H. Kheyrandish, and N. E. B. Cowern, Nucl. Instrum. Methods Phys. Res. B **237**, 131 (2005).
[5] B. Sadigh, T. J. Lenosky, M. Caturla, A. A. Quong, L. X. Benedict, T. D. de la Rubia, M. M. Giles, M. Foad, C. D. Spataru, and S. G. Louie, Appl. Phys. Lett. **80**, 4738 (2002).
[6] T. Alzanki, R. Gwilliam, N. Emerson, and B. J. Sealy, Appl. Phys. Lett. **85**, 1979 (2004).
[7] T. Alzanki, Ph.D. thesis, University of Surrey, 2004.
[8] P. Kringhoj, A. N. Larsen, and S. Y. Shirayev, Phys. Rev. Lett. **76**, 3372 (1996).
[9] J. Zangenberg, Ph.D. thesis, University of Aarhus, 2003.
[10] N. S. Bennett, A. J. Smith, B. Colombeau, R. Gwilliam, N. E. B. Cowern, and B. J. Sealy, Mater. Sci. Eng., B **124–125**, 305 (2005).
[11] Y. Sasaki, K. Itoh, E. Inoue, S. Kishi, and T. Mitsuishi, Solid-State Electron. **31**, 5 (1988).
[12] M. L. Lee, E. A. Fitzgerald, M. T. Bulsara, M. T. Currie, and A. Lochtefeld, J. Appl. Phys. **97**, 1 (2005).
[13] B. J. Sealy, A. J. Smith, T. Alzanki, N. Bennett, L. Li, C. Jeynes, B. Colombeau, E. J. H. Collart, N. G. Emerson, R. M. Gwilliam, and N. E. B. Cowern, *Proceedings of the Sixth International Workshop on Junction Technology* (IEEE, Shanghai, 2006).
[14] Y. K. Yeo, R. L. Hengehold, and D. W. Elsaesser, J. Appl. Phys. **61**, 5070 (1987).
[15] J. E. Dijkstra and W. Th. Wenckebach, J. Appl. Phys. **85**, 1587 (1999).
[16] S. Gannavaram, N. Pesovic, and C. Ozturk, Tech. Dig. - Int. Electron Devices Meet. **2000**, 437.
[17] T. Sanuki, A. Oishi, Y. Morimasa, S. Aota, T. Kinoshita, R. Hasumi, Y. Takegawa, K. Isobe, H. Yoshimura, M. Iwai, K. Sunouchi, and T. Noguchi, Tech. Dig. - Int. Electron Devices Meet. **2003**, 65.
[18] J. W. Matthews and A. E. Blakeslee, J. Cryst. Growth **27**, 118 (1974).

Downloaded 30 Jan 2008 to 136.206.1.17. Redistribution subject to AIP license or copyright; see http://apl.aip.org/apl/copyright.jsp